

# Inter-pocket pairing and gap symmetry in Fe-based superconductors with only electron pockets

M. Khodas<sup>1</sup> and A. V. Chubukov<sup>2</sup>

<sup>1</sup>*Department of Physics and Astronomy,  
University of Iowa, Iowa City, Iowa 52242, USA*

<sup>2</sup>*Department of Physics, University of Wisconsin, Madison, Wisconsin 53706, USA*

(Dated: February 28, 2012)

## Abstract

Pairing symmetry in recently discovered Fe-based metallic superconductors  $\text{AFe}_2\text{Se}_2$  ( $\text{A} = \text{K}, \text{Rb}, \text{Cs}$ ) with high transition temperature  $T_c \sim 40$  K is currently a subject of intensive debates. These systems contain only electron pockets, according to photoemission, and differ from the majority of Fe-based superconductors in which both electron and hole pockets are present. Both  $d$ -wave and  $s$ -wave pairing symmetries have been proposed for  $\text{AFe}_2\text{Se}_2$ , but a  $d$ -wave gap generally has nodes, while experiments clearly point to no-nodal behavior, and a conventional  $s$ -wave gap is inconsistent with the observation of the neutron resonance below  $T_c$ . We argue that current theories of pairing in such systems are incomplete and must include not only intra-pocket pairing condensate but also inter-pocket condensate made of fermions belonging to different electron pockets. We analyze the interplay between intra-pocket and inter-pocket pairing depending on the ellipticity of electron pockets and the strength of their hybridization and show that hybridization brings the system into a new  $s^{+-}$  state, in which the gap changes sign between hybridized pockets. This state has the full gap and at the same time supports spin resonance, in agreement with the data. Near the boundary of  $s^{+-}$  state we found a long-thought  $s + id$  state which breaks time-reversal symmetry.

**Introduction:** High-temperature superconductivity in Fe-pnictides has been discovered in 2008 (Ref. [1]) and almost instantly made to the top of the list of the most relevant issues for the physics community [2–5]. The interest in Fe-pnictides and Fe-chalcogenides, which display similar behavior, is two-fold. On one hand, these materials hold a strong potential for practical applications, on the other they display superconducting properties which does not fit into conventional classification scheme of superconductivity. In this scheme, *s*-wave superconductors have a gap of one sign and no nodes, *d*-wave superconductors have a sign-changing gap and line nodes (unless a *d*-wave state breaks time-reversal symmetry [6]), etc. For Fe-based superconductors (FeSCs), photoemission, penetration depth, thermal conductivity, neutron scattering, tunneling, and other experiments done on weakly/moderately doped systems show that the gap is *s*-wave, yet it very likely changes sign, and even has nodes in some materials.

The sign-changing *s*-wave superconductivity is generally understood as the consequence of complex geometry of the Fermi surface (FS), which in FeSCs consists of hole and electron pockets located in separate regions of the Brillouin zone, and of the competition between intra-pocket and inter-pocket interactions, both originating from electron - electron Coulomb repulsion. Intra-pocket repulsion is detrimental to an *s*-wave superconductivity, but inter-pocket repulsion supports *s*-wave superconductivity in which the gap changes sign between hole and electron pockets. When inter-pocket interaction wins, the system develops a "plus-minus" *s*-wave gap [7, 8] when intra-pocket interaction wins, *s*-wave superconductivity still develops, but the gap acquires variations along electron pockets to minimize the effect of intra-pocket repulsion [2, 9], and develops nodes when these variations become large.

This scenario works reasonably well for weakly/moderately doped FeSCs, in which both hole and electron pockets are present. Recently, however, superconductivity with rather high  $T_c \sim 40$  K has been discovered [10, 11] in  $A_x\text{Fe}_{2-y}\text{Se}_2$  ( $\text{AFe}_2\text{Se}_2$ ) with  $A = \text{K, Rb, Cs}$ , which have only electron pockets, according to photoemission [12]. The electronic states near would be hole pockets have energy of at least 60 meV and are unlikely to contribute to superconductivity, i.e., the reasoning based on the interaction between hole and electron pockets cannot be applied to these systems.

Superconductivity in  $\text{AFe}_2\text{Se}_2$  has been studied recently by several groups [13–20]. In the Fe-only Brillouin zone, electron pockets are located near  $(0, \pi)$  and  $(\pi, 0)$  (here and below we set interatomic spacing  $a = 1$ ). If we just replace intra-pocket hole-electron interaction

by intra-pocket interaction between electron pockets, we find that a gap must change sign between  $(0, \pi)$  and  $(\pi, 0)$  pockets. Such a gap is antisymmetric with respect to interchange between  $X$  and  $Y$  coordinates and hence has  $d$ -wave symmetry [13–16]. Taken at a face value, this gap is of "plus-minus" type and has no nodes. However, no-nodal  $d$ -wave gap is rather fragile and was argued [17] to acquire symmetry-related nodes once one includes the hybridization between the electron pockets due to an additional interaction via a Se. The data on  $\text{AFe}_2\text{Se}_2$ , however, show that the gap has no nodes [21–23]. Several groups argued [17–20] that a no-nodal behavior indicates that the gap in  $\text{AFe}_2\text{Se}_2$  must be  $s$ -wave, but a conventional  $s$ -wave gap is inconsistent with recent observation of the spin resonance below  $T_c$  in  $\text{Rb}_x\text{Fe}_{2-y}\text{Se}_2$  (Ref. [24]).

In this communication, we show that nodeless superconductivity consistent with the spin resonance in fact appears quite naturally in a situation when only electron pockets are present. We argue that complete theory of superconductivity in such geometry should include on equal footings a pairing condensate made out of fermions on the same pocket (intra-pocket pairing) and a pairing condensate made out of fermions on different pockets (inter-pocket pairing). Inter-pocket pairing has been earlier discussed for other systems, most recently for inter-valley pairing in graphene [25]. It was discussed in early days of Fe-pnictides regarding a possible spin-triplet, even-parity pairing in weakly doped FeSCs [26,27], but was not considered in previous works on the pairing in FeSCs with only electron pockets. We argue that, whenever two FS pockets cross upon folding and split due to hybridization, inter-pocket pairing must be included on equal footings with intra-pocket pairing. For  $\text{AFe}_2\text{Se}_2$  inter-pocket pairing is particularly important because both hybridization *and* ellipticity are small [17], but we argue that it is generally relevant to the pairing in the presence of hybridization because intra-pocket pairing for non-hybridized fermions becomes inter-pocket pairing for hybridized fermions, and vice versa (see below).

We show that the interplay between intra- and inter-pocket pairing in the standard model leads to a competition between  $d$ -wave and  $s$ -wave states. We find three phases, depending on the degree of eccentricity of electron pockets and the strength of the hybridization – an  $s$ -wave, a  $d \pm is$  state which breaks time-reversal symmetry, and a  $d$ -wave state. In  $s$ -wave and  $s + id$  states, all states are gapped. In a  $d$ -wave state, there are nodes, but unusual ones – they form vertical loops centered  $k_z = \pi/2$ . In some range of parameters, loops collapse and a  $d$ -wave state also becomes nodeless. The  $s$ -wave is of plus-minus type – the gaps on

hybridized FSs have opposite signs. Such state has been earlier proposed phenomenologically by I. Mazin [17]. Our results explain microscopic mechanism of such  $s^+$ –superconductivity.

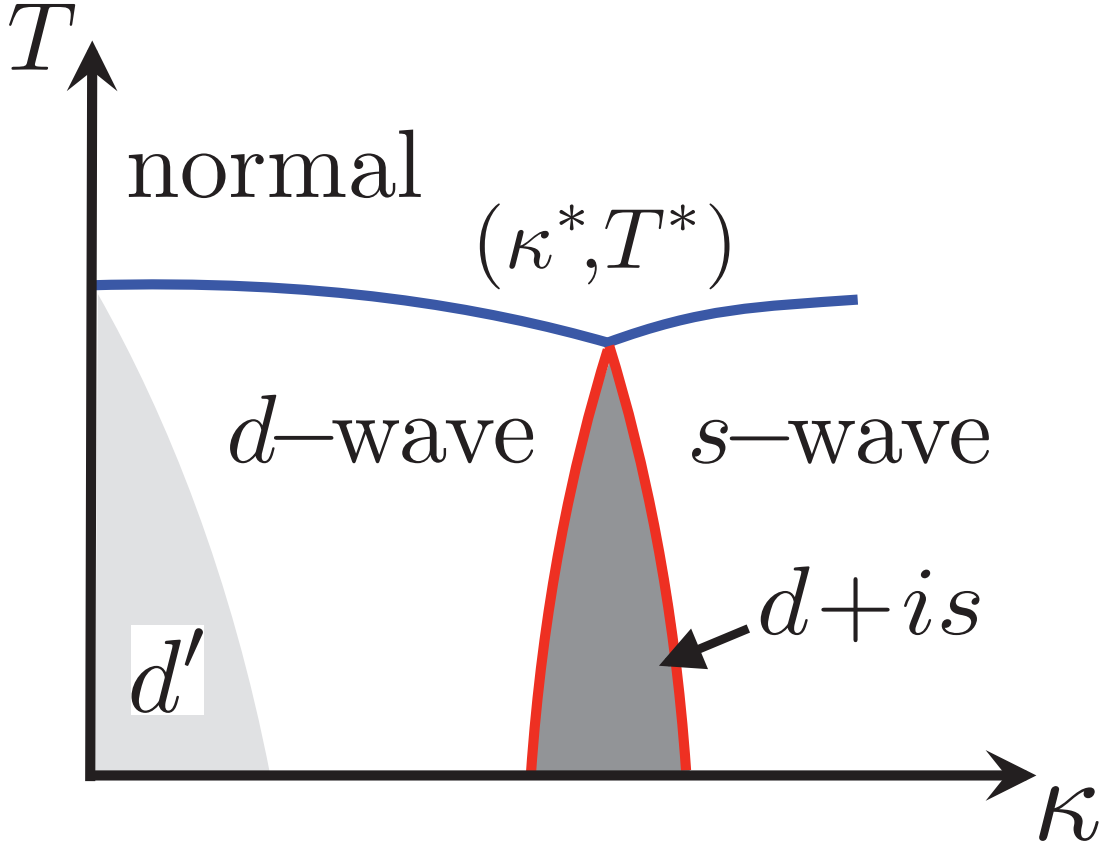


FIG. 1: The phase diagram in  $(\kappa, T)$ -plane for Fe-based superconductors with only electron pockets. Two solid and almost horizontal lines (blue) separates normal and superconducting phases. Four solid lines of second order phase transition converge at the tetra-critical point  $(\kappa^*, T^*)$ . The  $s + id$  phase with broken time reversal symmetry is shown by the dark (grey) shaded area confined by two solid (red) almost vertical lines. The two neighboring superconducting phases at  $\kappa < (>)\kappa^*$  have  $d(s)$ -wave ordering respectively. In the  $d'$  region the excitation spectrum is fully gapped even though the order parameter has a  $d$ -wave symmetry.

**Methods:** We consider the low-energy physics of FeSCs with only electron pockets within a 2D model of fermions near  $(0, \pi)$  and  $(\pi, 0)$ , interacting either directly, or via a pnictogen/chalcogen. The direct interaction is a momentum-conserving process, up to a lattice momentum in the Fe-zone,  $2\pi$ , the indirect one has excess momentum  $\mathbf{Q} = (\pi, \pi)$  taken by pnictide/chalcogenide. This last interaction then hybridizes the two electron pock-

ets and also gives rise to additional 4-fermion interactions with excess momentum  $\mathbf{Q}$ . We show that the hybridization is overly relevant while additional interaction does not play much role. The hybridization in  $\text{AFe}_2\text{Se}_2$  actually involves momentum  $(\pi, \pi, \pi)$  because of body-centered tetragonal structure of these materials, i.e., hybridized fermions belong to different planes separated by  $k_z = \pi$  [17, 28]. To simplify the presentation, we first consider hybridization for a simple tetragonal structure, for which hybridized fermions have the same  $k_z$ , and then extend the analysis to body-centered tetragonal structure.

Let  $c_{\mathbf{k}}^\dagger$  be a creation operator for electrons at  $(0, \pi)$ , and  $f_{\mathbf{k}}^\dagger = c_{\mathbf{k}+\mathbf{Q}}^\dagger$  is a creation operator of electrons at  $(\pi, 0)$ . The quadratic part of the Hamiltonian  $H = H_2 + H_{int}$  is

$$H_2 = \sum_{\mathbf{k}} \epsilon_{\mathbf{k}}^c c_{\mathbf{k}}^\dagger c_{\mathbf{k}} + \sum_{\mathbf{k}} \epsilon_{\mathbf{k}}^f f_{\mathbf{k}}^\dagger f_{\mathbf{k}} + \sum_{\mathbf{k}} \lambda \left[ c_{\mathbf{k}}^\dagger f_{\mathbf{k}} + f_{\mathbf{k}}^\dagger c_{\mathbf{k}} \right], \quad (1)$$

where the first two terms describe fermion dispersion, and the last term describes the hybridization, i.e., the process with excess momentum  $\mathbf{Q}$  taken by Se. The two elliptical FSs are defined by  $\epsilon_{\mathbf{k}}^{c(f)} = \epsilon_F$ . We approximate fermion excitations near these FSs by

$$\epsilon_{\mathbf{k}}^c = v_F(\phi)(k - k_F(\phi)), \quad \epsilon_{\mathbf{k}}^f = v_F(\phi + \pi/2)(k - k_F(\phi + \pi/2)), \quad (2)$$

where  $\phi$  is the angle along each of the the FSs counted from the  $x$ -axis. By virtue of tetragonal symmetry,  $v_F(\phi) = v_F(1 + a \cos 2\phi)$  and  $k_F(\phi) = k_F(1 + b \cos 2\phi)$ . The anisotropy of the Fermi velocity does not play a major role in our analysis, but the eccentricity of the FS (the parameter  $b$ ) is overly relevant. Both  $b$  and  $\lambda/(v_F k_F)$  are small for  $\text{AFe}_2\text{Se}_2$  (Ref.[17]), but their ratio  $\kappa = \lambda/(v_F k_F |b|)$  can be arbitrary. For simplicity, we assume that  $\lambda$  is independent on the direction of  $\mathbf{k}$ . A more complex form of  $\lambda(\mathbf{k})$  will affect our results quantitatively but not qualitatively.

The interaction Hamiltonian generally involves direct, momentum-conserving, 4-fermion interactions, and interactions via a pnictide or a chalcogenide (Se in our case) with excess momentum  $\mathbf{Q}$ . The four direct interactions are

$$\begin{aligned} H_1 &= \frac{u_1}{2} \int d\mathbf{x} \left( c_{\sigma}^\dagger f_{\sigma'}^\dagger f_{\sigma'} c_{\sigma} + f_{\sigma}^\dagger c_{\sigma'}^\dagger c_{\sigma'} f_{\sigma} \right) \\ H_2 &= \frac{u_2}{2} \int d\mathbf{x} \left( c_{\sigma}^\dagger f_{\sigma'}^\dagger c_{\sigma'} f_{\sigma} + f_{\sigma}^\dagger c_{\sigma'}^\dagger f_{\sigma'} c_{\sigma} \right) \\ H_3 &= \frac{u_3}{2} \int d\mathbf{x} \left( c_{\sigma}^\dagger c_{\sigma'}^\dagger f_{\sigma'} f_{\sigma} + f_{\sigma}^\dagger f_{\sigma'}^\dagger c_{\sigma'} c_{\sigma} \right) \\ H_4 &= \frac{u_4}{2} \int d\mathbf{x} \left( c_{\sigma}^\dagger c_{\sigma'}^\dagger c_{\sigma'} c_{\sigma} + f_{\sigma}^\dagger f_{\sigma'}^\dagger f_{\sigma'} f_{\sigma} \right) \end{aligned} \quad (3)$$

$H_1$  and  $H_2$  are inter-band density-density and exchange interactions, interaction,  $H_4$  is the intra-band density-density interaction, and  $H_3$  describes the umklapp pair-hopping processes. We assume that all interactions are repulsive and angle-independent. The interaction with excess momentum  $\mathbf{Q}$  is

$$H_{\mathbf{Q}} = w_1 \int d\mathbf{x} (c_{\sigma}^{\dagger} f_{\sigma} + f_{\sigma}^{\dagger} c_{\sigma}) (c_{\sigma'}^{\dagger} c_{\sigma'} + f_{\sigma'}^{\dagger} f_{\sigma'}) . \quad (4)$$

Other interactions with  $\mathbf{Q}$  vanish without time-reversal symmetry breaking.

The quadratic Hamiltonian can be diagonalized by unitary transformation to new operators  $a_{\mathbf{k}} = c_{\mathbf{k}} \cos \theta_{\mathbf{k}} + f_{\mathbf{k}} \sin \theta_{\mathbf{k}}$ ,  $b_{\mathbf{k}} = -c_{\mathbf{k}} \sin \theta_{\mathbf{k}} + f_{\mathbf{k}} \cos \theta_{\mathbf{k}}$  with

$$\sin 2\theta_{\mathbf{k}} = \frac{\lambda}{\sqrt{\lambda^2 + (\epsilon_{\mathbf{k}}^c - \epsilon_{\mathbf{k}}^f)^2/4}} , \quad \cos 2\theta_{\mathbf{k}} = \frac{(\epsilon_{\mathbf{k}}^c - \epsilon_{\mathbf{k}}^f)}{2\sqrt{\lambda^2 + (\epsilon_{\mathbf{k}}^c - \epsilon_{\mathbf{k}}^f)^2/4}} . \quad (5)$$

In terms of new operators,

$$H_2 = \sum_{\mathbf{k}} E_{\mathbf{k}}^a a_{\mathbf{k}}^{\dagger} a_{\mathbf{k}} + \sum_{\mathbf{k}} E_{\mathbf{k}}^b b_{\mathbf{k}}^{\dagger} b_{\mathbf{k}} \quad (6)$$

with

$$E_{\mathbf{k}}^{a,b} = \frac{1}{2} (\epsilon_{\mathbf{k}}^c + \epsilon_{\mathbf{k}}^f) \pm \left[ \lambda^2 + (\epsilon_{\mathbf{k}}^c - \epsilon_{\mathbf{k}}^f)^2/4 \right]^{1/2} . \quad (7)$$

In our notations,  $(\epsilon_{\mathbf{k}}^c + \epsilon_{\mathbf{k}}^f)/2 \approx \epsilon_F + v_F(k - k_F) = \epsilon_F + \xi$ , and  $(\epsilon_{\mathbf{k}}^c - \epsilon_{\mathbf{k}}^f)/2 \approx v_F k_F b \cos 2\phi$ , such that  $E_{\mathbf{k}}^{a,b} - \epsilon_F = \xi \pm \lambda (1 + \cos^2 2\phi/\kappa^2)^{1/2}$ ,  $\cos^2 2\theta = \cos^2 2\phi/(\kappa^2 + \cos^2 2\phi)$ , and  $\sin^2 2\theta = \kappa^2/(\kappa^2 + \cos^2 2\phi)$ .

*Qualitative reasoning:* The interplay between intra-pocket and inter-pocket pairing, and between  $d$ -wave and  $s$ -wave gap symmetry can be understood by considering the limits of small and large  $\kappa$  (Fig. 2). At  $\kappa \rightarrow 0$  the hybridization vanishes, i.e.,  $c$  and  $f$  are primary operators. For elliptical pockets, intra-pocket Cooper susceptibility is the largest one, and when  $u_3 > u_4$ , the system develops a conventional pairing instability with  $\Delta_c = \langle c_{\uparrow}^{\dagger} c_{\downarrow}^{\dagger} \rangle$  and  $\Delta_f = \langle f_{\uparrow}^{\dagger} f_{\downarrow}^{\dagger} \rangle$  and  $\Delta_f = -\Delta_c$  (Fig. 2a). This solution is antisymmetric with respect to  $c \leftrightarrow f$  and hence is  $d$ -wave. Consider next the opposite limit of large  $\kappa$ . Now  $a$  and  $b$  are primary fermion operators, and the FSs of  $a$  and  $b$  fermions are well separated in the momentum space (Fig. 2b). The leading pairing instability is again a conventional intra-pocket one, and the gaps  $\Delta_a = \langle a_{\uparrow}^{\dagger} a_{\downarrow}^{\dagger} \rangle$  and  $\Delta_b = \langle b_{\uparrow}^{\dagger} b_{\downarrow}^{\dagger} \rangle$  obey  $\Delta_a = -\Delta_b$ . This gap, however, is a sign-changing  $s$ -wave rather than  $d$ -wave. To see this, we note that at large  $\kappa$ ,  $a_{\uparrow}^{\dagger} a_{\downarrow}^{\dagger} - b_{\uparrow}^{\dagger} b_{\downarrow}^{\dagger} = c_{\uparrow}^{\dagger} f_{\downarrow}^{\dagger} + f_{\uparrow}^{\dagger} c_{\downarrow}^{\dagger}$ , i.e., the solution  $\Delta_a = -\Delta_b$  corresponds to non-zero  $\langle c_{\uparrow}^{\dagger} f_{\downarrow}^{\dagger} + f_{\uparrow}^{\dagger} c_{\downarrow}^{\dagger} \rangle$ . The latter combination

is symmetric with respect to  $c \leftrightarrow f$  and hence is an  $s$ -wave. We also see that, in terms of original fermions, the pairing condensate is now the inter-pocket one – it is made out of fermions belonging to different pockets. What happened with the  $d$ -wave solution? At large  $\kappa$  we have  $c_{\uparrow}^{\dagger}c_{\downarrow}^{\dagger} - f_{\uparrow}^{\dagger}f_{\downarrow}^{\dagger} = -(a_{\uparrow}^{\dagger}b_{\downarrow}^{\dagger} + b_{\uparrow}^{\dagger}a_{\downarrow}^{\dagger})$ . Hence, in terms of  $a$  and  $b$  operators,  $d$ -wave pairing now becomes inter-pocket pairing. We see therefore that intra-pocket pairing in terms of one set of fermions corresponds to inter-pocket pairing in terms of the other set. Since the pairing symmetry changes from a  $d$ -wave to an  $s$ -wave between small and large  $\kappa$ , and because within the original set the former is an intra-pocket pairing and the latter is an inter-pocket pairing, one *must* include the two pairings on an equal footing in order to describe the transformation from  $d$ - to  $s$ -wave symmetry.

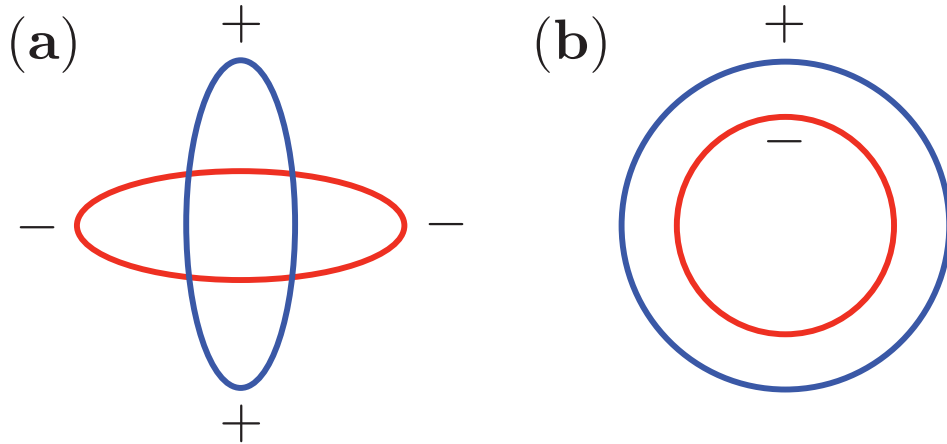


FIG. 2: The structure of superconducting gap at small and large  $\kappa$ , which is the ratio of the hybridization and the degree of ellipticity of the electron pockets. At the smallest  $\kappa$  (panel a), the gap has different sign on the original FS pockets and is  $d$ -wave because it is antisymmetric with respect to rotation by  $90^\circ$ . At large  $\kappa$  (panel b), the gap again changes sign, but now between hybridized FS pockets. This gap is symmetric with respect to  $90^\circ$  rotation and is therefore an  $s$ -wave.

It is natural to analyze the pairing in terms of new  $a$  and  $b$  fermions because the Hamiltonian, Eq. (1), is then quadratic at all values of  $\kappa$ . We introduce intra- and inter-band pair creation operators,

$$J_{\pm}^{\dagger} = \frac{1}{2} (a^{\dagger}a^{\dagger} \pm b^{\dagger}b^{\dagger}) , \quad \tilde{J}_{\pm}^{\dagger} = \frac{1}{2} (a^{\dagger}b^{\dagger} \pm b^{\dagger}a^{\dagger}) . \quad (8)$$

The combinations  $J_+^\dagger$  and  $\tilde{J}_-^\dagger$  describe an ordinary, "plus-plus"  $s$ -wave pairing and spin-triplet, even parity inter-band pairing, respectively (the triplet channel is identical to the one considered in [26]). In our case, these two pairing channels are strongly repulsive, and we can safely omit them. The linear combinations of the other two components  $J_-^\dagger$  and  $\tilde{J}_+^\dagger$  describe  $s$ -wave pair creation operators

$$\frac{1}{2} \left( c_\sigma^\dagger f_{\sigma'}^\dagger + f_\sigma^\dagger c_{\sigma'}^\dagger \right) = \left[ \cos 2\theta \tilde{J}_+^\dagger + \sin 2\theta J_-^\dagger \right]_{\sigma\sigma'} \quad (9)$$

and  $d$ -wave pair creation operators

$$\frac{1}{2} \left( c_\sigma^\dagger c_{\sigma'}^\dagger - f_\sigma^\dagger f_{\sigma'}^\dagger \right) = \left[ \cos 2\theta J_-^\dagger - \sin 2\theta \tilde{J}_+^\dagger \right]_{\sigma\sigma'} , \quad (10)$$

where the angle  $\theta$  is defined in Eq. (5). The interaction, Eq. (3), can then be decomposed into an  $s$ -wave and  $d$ -wave channels,  $H_{int} = H_s + H_d$  with

$$H_s = -2u_s [s' J_-^\dagger + c' \tilde{J}_+^\dagger]_{\sigma\sigma'} [s J_- + c \tilde{J}_+]_{\sigma'\sigma} , \quad (11)$$

$$H_d = -2u_d [c' J_-^\dagger - s' \tilde{J}_+^\dagger]_{\sigma\sigma'} [c J_- - s \tilde{J}_+]_{\sigma'\sigma} , \quad (12)$$

where  $c \equiv \cos 2\theta$ ,  $c' \equiv \cos 2\theta'$ ,  $s \equiv \sin 2\theta$ ,  $s' \equiv \sin 2\theta'$  and  $2u_s = -u_1 - u_2$ ,  $2u_d = u_3 - u_4$ . We emphasize that the intra- and inter- band pairings enter Eqs. (11), (12) on equal footing. We also emphasize that  $J_-^\dagger$  describes a "plus-minus"  $s$ -wave pairing (different sign of the gaps on  $a$  and  $b$  FSs), hence our  $s$ -wave state is sign-changing  $s$ -wave. For circular electron pockets, the  $O(2)$  rotational symmetry in  $(c, f)$  space along with  $SU(2)$  spin symmetry requires [29]  $u_s = u_d = u$ . For weak ellipticity,  $u_d$  and  $u_s$  do not have to be identical, but remain close and we keep  $u_s = u_d = u$  for simplicity. A positive  $u$  is required for superconductivity. The interaction  $H_Q$  couples these two channels with plus-plus  $s$ -wave channel and spin-triplet channels which we already neglected, and does not play a role in our analysis.

*Ginzburg-Landau Functional:* To map a phase diagram in  $(\kappa, T)$ -plane we derive the Ginzburg-Landau Functional (GLF). We introduce order parameters  $\Delta_s$  and  $\Delta_d$  to decouple the interaction in two Cooper channels using the Hubbard-Stratonovitch identity, integrate over fermion fields and expand the effective action in powers of  $\Delta_s$  and  $\Delta_d$ . Carrying out the calculations (see [30]) we obtain

$$\begin{aligned} F_{GL} = & A_s |\Delta_s|^2 + A_d |\Delta_d|^2 + \frac{B_s}{2} |\Delta_s|^4 + \frac{B_d}{2} |\Delta_d|^4 \\ & + C |\Delta_s|^2 |\Delta_d|^2 + \frac{E}{2} ((\Delta_s \Delta_d^*)^2 + (\Delta_s^* \Delta_d)^2) . \end{aligned} \quad (13)$$



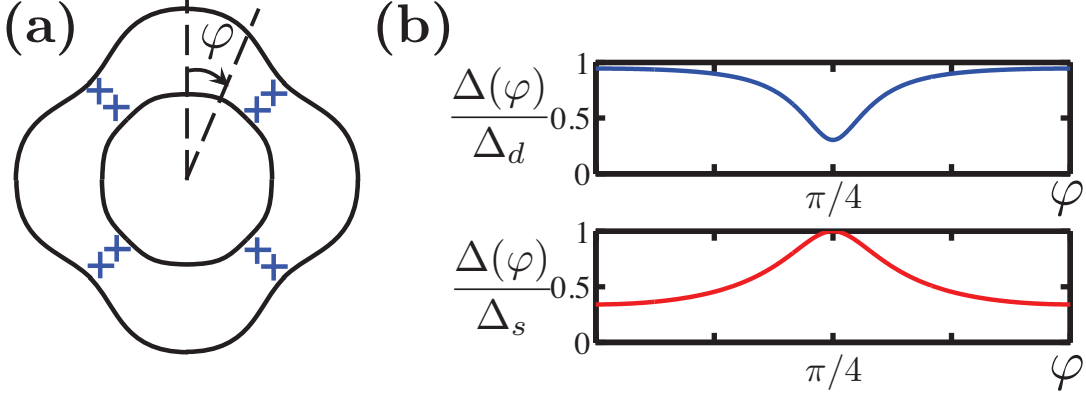


FIG. 3: a) The hybridized FSs at intermediate  $\kappa = O(1)$ . Crosses mark the location of the nodal points (zero energy states) in the  $d$ -wave phase. Upon approaching the boundary of  $d'$  phase in Fig.1, nodal points come closer and eventually collapse, leading to a  $d$ -wave state with a full gap. b) The modulation of the gap magnitude along the FSs for  $d$ -wave and  $s$ -wave states. Within our approximations, gap modulations along the two FSs are equivalent.

The transition to either  $s$ -wave or  $d$ -wave state is determined by  $A_s = 0$  or  $A_d = 0$ , whichever comes first. The lines  $A_s = 0$  and  $A_d = 0$  cross at some critical  $\kappa^*$ , at which  $T_c = T_c^*$ . The value of  $\kappa^*$  depends on  $T_c^*/\lambda$ . In  $\text{AFe}_2\text{Se}_2$ ,  $\lambda$  is a fraction of  $\epsilon_F$  and  $T_c^* \ll \epsilon_F$ , hence  $T_c^* \ll \lambda$ . In this limit, we obtained  $\kappa^* = 1/\sqrt{3}$  (in the other limit, which we consider for completeness in [30],  $\kappa^* = 1/\sqrt{2}$ ). The transition temperature is determined by  $\log \Lambda/T_c^* = 2/(uN_F)$ , where  $N_F = k_F/(2\pi v_F)$  is the density of states at the Fermi level and  $\Lambda \sim \epsilon_F$  is the upper cutoff. Near the critical  $\kappa$ , the first instability occurs at  $T_{c,s} = T_c^*(1 + \alpha(\kappa - \kappa^*))$  for  $\kappa > \kappa^*$  and at  $T_{c,d} = T_c^*(1 + \alpha(\kappa^* - \kappa))$  for  $\kappa < \kappa^*$ , where  $\alpha = 3\sqrt{3}/(2uN_F)$  (see Fig. 1).

The transition from a  $d$ -wave order at  $\kappa < \kappa^*$  to an  $s$ -wave order at  $\kappa > \kappa^*$  is determined by the interplay between fourth-order terms in Eq. (13). The transition can be either first order or continuous, via an intermediate phase where both orders are present. At  $T = T_c^*$  we obtained  $B_s = B_d = B = \frac{5}{8}I_0$ ,  $C = \frac{3}{8}I_0$ , and  $E = C/2$ , where  $I_0 = 7\zeta(3)/8\pi^2(T_c^*)^2$ . We see that  $E > 0$  and  $B + E > C$ . An elementary analysis then shows that the transition from  $d$  to  $s$  involves an intermediate phase in which the two orders mix with relative phase  $\pm\pi/2$ . This is long-thought  $s \pm id$  state [31]. The system chooses either  $s + id$  or  $s - id$  state and by this breaks time-reversal symmetry. The boundaries of this intermediate phase are set by  $T_{s+id} = T_c^*(1 - \beta|\kappa - \kappa^*|)$ , where  $\beta = 6\sqrt{3}/(uN_F)$ . We emphasize again that the transition

from  $s$  to  $d$  and the existence of the intermediate phase are both the consequences of the competition between intra-pocket and inter-pocket pairing (we recall that  $2\Delta_s = c_{\uparrow}^{\dagger}f_{\downarrow}^{\dagger} + f_{\uparrow}^{\dagger}s_{\downarrow}^{\dagger}$ ,  $2\Delta_d = c_{\uparrow}^{\dagger}c_{\downarrow}^{\dagger} - f_{\uparrow}^{\dagger}f_{\downarrow}^{\dagger}$ ).

*The excitations:* Experiments on  $\text{AFe}_2\text{Se}_2$  show [10, 11] that fermion excitations are fully gapped in the superconducting state. In our theory this holds in the  $s$ -wave state and in the intermediate  $s \pm id$  state. In the  $d$ -wave state, the excitation spectrum is given [30]:

$$\omega_{\pm}^2 = |\Delta_d|^2 \cos^2 2\theta + \left( \sqrt{\xi^2 + |\Delta_d|^2 \sin^2 2\theta} \pm \frac{\lambda}{\sin 2\theta} \right)^2, \quad (14)$$

where, we remind,  $\xi = (\epsilon_c + \epsilon_f)/2 - \epsilon_F \approx v_F(k - k_F)$ . The dispersion  $\omega_-$  has nodes (solutions with  $\omega_{\pm} = 0$ ) along the diagonal directions where  $\cos 2\theta = 0$ , as it should be for a  $d$ -wave superconductor. However, the nodal points are located in between  $a$  and  $b$  FSs, as shown in Fig. 3a, i.e., along the  $a$  and  $b$  FSs excitations do not have nodes. This is another consequence of the presence of inter-pocket pairing. We plot the dispersions in  $s$ - and  $d$ -wave states in Fig. 3b. We furthermore see from (14) that nodes in the  $d$ -wave state exist only if  $|\Delta_d| < \lambda$ , otherwise the second term in the r.h.s of (14) does not vanish even when  $\xi = 0$ . The condition  $|\Delta_d| = \lambda$  then sets the boundary of the *nodeless*  $d$ -wave state (we dubbed this state as  $d'$  on Fig. 1). For a tetragonal system, realistic  $\lambda$  are larger than  $\Delta_d$ , but we will see below that the presence of  $d'$  state on the phase diagram is relevant to the structure of the nodes in the  $d$ -wave phase of  $\text{AFe}_2\text{Se}_2$ .

*Specifics of  $\text{AFe}_2\text{Se}_2$ :* The hybridization of electron pockets in  $\text{AFe}_2\text{Se}_2$  is involved because of the body-centered tetragonal structure of these materials [10]. The two hybridized electron FSs differ by  $k_z = \pi$  and are rotated by  $\pi/2$  (see Fig. 4a-c and Refs.[17, 28]). For  $k_z = 0$  and  $k_z = \pi$ , the FS in the folded zone consists of co-aligned ellipses (Fig. 4d-f), the pair near  $(\pi, \pi)$  at  $k_z = 0$  is identical to the one near  $(-\pi, \pi)$  at  $k_z = \pi$ . At  $k_z = \pm\pi/2$ , the pairs at  $(\pi, \pi)$  and  $(-\pi, \pi)$  are identical already at the same  $k_z$ .  $s$ -wave and  $d$ -wave gaps differ in whether the gap on the larger ellipsis retains sign or changes sign between  $k_z = 0$  and  $k_z = \pi$  (Fig. 4g-h). Which of the two states is realized then depends on the behavior around  $k_z = \pi/2$  where our 2D analysis is applicable [32]. Using our 2D results, we find that a  $d$ -wave state, with intra-pocket pairing in terms of original fermions, wins at small  $\kappa$ , and an  $s$ -wave state, with intra-pocket pairing in terms of new, hybridized fermions, wins at large  $\kappa$ , and there is  $s + id$  phase in between. In a  $d$ -wave state nodal points exist near  $k_z = \pi/2$  (again away from the FSs), but not near  $k_z = 0$  and  $k_z = \pi$ , where the FSs at

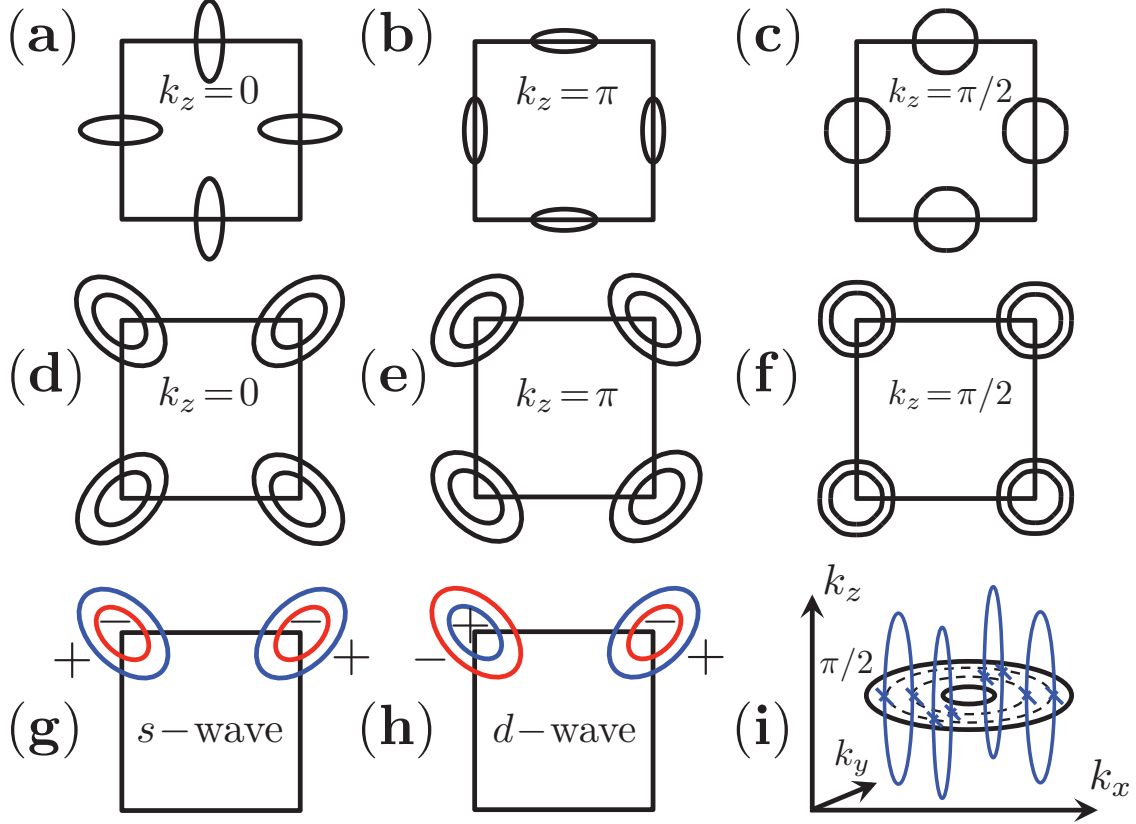


FIG. 4: The structure of electronic states and the superconducting gap in  $\text{AFe}_2\text{Se}_2$  which have body-centered tetragonal structure. Panels a-c – electron pockets in the unfolded Brillouin zone for different  $k_z$ . Panels d-f – same in the folded zone. Note that the two ellipses at each corner remain co-axial and rotate by  $90^\circ$  between  $k_z = 0$  and  $k_z = \pi$ . The hybridized FSs at  $k_z = \pi/2$  would be circular if one restricted with quadratic dispersion, as in (2) but acquire 4-fold variation due to higher-order terms in the dispersion. Panels g-h –  $s$ -wave and  $d$ -wave gap structure near  $k_z = 0$  and  $k_z = \pi$ . Panel i – the location of the nodes at  $k_z \approx \pi/2$ . The nodal points form vertical loops (only two are shown for clarity). If hybridized FSs at  $\pi/2$  are two circles, the crosses extend and form lines in  $(k_x, k_y)$  plane (dashed lines in the Figure).

the same  $k_x, k_y$  in the folded zone are co-axial ellipses of different sizes, and hybridization can only cause minor variations of originally angle-independent gap (this behavior is the same as in  $d'$  region in Fig. 1). Consequently the nodes in the  $d$ -wave state form vertical loops centered at  $k_z = \pi/2$  (Fig. 4i). Vertical loop nodes, although of different kind, have been earlier suggested on phenomenological grounds [33, 34], but have not been computed

microscopically.

**Outlook**– In this work we argued that the pairing in recently discovered Fe-based superconductors  $\text{AFe}_2\text{Se}_2$  ( $A = \text{K, Rb, Cs}$ ) with only electron pockets must necessary include inter-band pairing correlations between fermions belonging to different pockets. We demonstrated that the interplay between intra-pocket and inter-pocket pairing leads, already within a "standard model", to a transition from  $d$ -wave pairing at small degree of hybridization to an  $s$ -wave pairing at larger hybridization. In terms of hybridized fermions  $d$ -wave is inter-pocket pairing and  $s$ -wave is intra-pocket pairing, in terms of original fermions it is other way around. We found that the transformation from  $d$  to  $s$  is continuous and there is an intermediate, long-thought  $s \pm id$  mixed phase with broken time reversal symmetry. Fermion excitations in  $s$ -wave and  $s + id$  states are fully gapped, and  $s$ -wave gap is of  $s^{+-}$  type, with sign change between hybridized pockets. Such an  $s$ -wave gap should give rise to a spin resonance below  $T_c$  [17, 35, 36]. The absence of nodes and the existence of a spin resonance are consistent with the data [10, 24]. A  $d$ -wave state contains vertical loop nodes, the size of the loop depends on the ratio of hybridization and the gap amplitude, and is small for small hybridization. The normal state,  $s$ -wave,  $d$ -wave, and  $s \pm id$  state all merge at the tetra-critical point on the phase diagram. We encourage photoemission studies of fermion excitations in  $\text{AFe}_2\text{Se}_2$  around  $k_z = \pi/2$  and *away* from the FS to determine whether the pairing state is  $s$ -wave or  $d$ -wave, and studies of potential time reversal-symmetry breaking below  $T_c$ . We also encourage the analysis of the effects of inter-band pairing in other Fe-based superconductors.

## Acknowledgements

We are thankful to I. Mazin for numerous discussions, careful reading of the manuscript, and useful suggestions. We acknowledge helpful discussions with A. Bernevig, R. Fernandes, P. Hirschfeld, S. Graser, I. Eremin, K. Kuroki, D-H. Lee, S. Maiti, D. Scalapino, R. Thomale, and M. Vavilov. This work was supported by University of Iowa (M.K.) and NSF-DMR-0906953 (A.C). A support from Humboldt foundation (A.C) is gratefully acknowledged. M.K and A.C jointly identified the problem, performed the analysis and wrote the paper.

Correspondence should be addressed to A.C.

---

- <sup>1</sup> Y. Kamihara, T. Watanabe, M. Hirano, H. Hosono, J. Am. Chem. Soc. **130**, 3296(2008).
- <sup>2</sup> A.F. Kemper, T.A. Maier, S. Graser, H-P. Cheng, P.J. Hirschfeld and D.J. Scalapino, New J. Phys. **12**, 073030(2010).
- <sup>3</sup> P.J. Hirschfeld, M.M. Korshunov, and I.I. Mazin, Rep. Prog. Phys. **74**, 124508 (2011).
- <sup>4</sup> A.V. Chubukov, Annul. Rev. Cond. Mat. Phys. **3**, 13.113.36, (2012).
- <sup>5</sup> H.H. Wen and S. Li, Annu. Rev. Condens. Matter Phys., **2**, 121 (2011).
- <sup>6</sup> for the latest see R. Nandkishore, L. Levitov and A. Chubukov, Nature Phys. **8**, 158163 (2012).
- <sup>7</sup> I. I. Mazin, D. J. Singh, M. D. Johannes, and M. H. Du, Phys. Rev. Lett. **101**, 057003 (2008).
- <sup>8</sup> K. Kuroki, S. Onari, R. Arita, H. Usui, Y. Tanaka, H. Kontani, and H. Aoki, Phys. Rev. Lett. **101**, 087004 (2008).
- <sup>9</sup> A. V. Chubukov, M. G. Vavilov, A. B. Vorontsov, Phys. Rev. B **80**, 140515(R)(2009).
- <sup>10</sup> J. Guo, S. Jin, G. Wang, S. Wang, K. Zhu, T. Zhou, M. He, and X. Chen, Phys. Rev. B **82**, 180520(R) (2010).
- <sup>11</sup> For most recent results see Y. Liu, Z. C. Li, W. P. Liu, G. Friemel, D. S. Inosov, R. E. Dinnebier, Z. J. Li, C. T. Lin, arXiv:1201.0902 and referennces therein.
- <sup>12</sup> T. Qian, X.-P. Wang, W.-C. Jin, P. Zhang, P. Richard, G. Xu, X. Dai, Z. Fang, J.-G. Guo, X.-L. Chen, H. Ding, Phys. Rev. Lett. **106**, 187001 (2011).
- <sup>13</sup> T.A. Maier, S. Graser, P. J. Hirschfeld, and D. J. Scalapino, Phys. Rev. B **83**, 100515(R) (2011)
- <sup>14</sup> T. Das and A. V. Balatsky, Phys. Rev. B **84**, 014521 (2011); Phys. Rev. B **84**, 115117 (2011)
- <sup>15</sup> F. Wang, F. Yang, M. Gao, Z.-Y. Lu, T. Xiang and D.-H. Lee, Europhys. Lett. **93** 57003 (2011).
- <sup>16</sup> S. Maiti, M. M. Korshunov, T. A. Maier, P. J. Hirschfeld, and A. V. Chubukov, Phys. Rev. B **84**, 224505 (2011); Phys. Rev. Lett. **107**, 147002 (2011).
- <sup>17</sup> I.I. Mazin, Phys. Rev. B **84**, 024529 (2011).
- <sup>18</sup> R. Yu, P. Goswami, Q. Si, P. Nikolic, J.-X. Zhu, arXiv:1103.3259.
- <sup>19</sup> C. Fang, Y.-L. Wu, R. Thomale, B. A. Bernevig, J. Hu, Physical Review X **1**, 011009 (2011)
- <sup>20</sup> T. Saito, S. Onari, and H. Kontani Phys. Rev. B **83**, 140512(R) (2011).
- <sup>21</sup> Y. Zhang, L. X. Yang, M. Xu, Z. R. Ye, F. Chen, C. He, J. Jiang, B. P. Xie, J. J. Ying, X. F. Wang, X. H. Chen, J. P. Hu, D. L. Feng, Nature Materials **10**, 273-277 (2011).

- <sup>22</sup> D. Mou, S. Liu, X. Jia, J. He, Y. Peng, L. Zhao, Li Yu, G. Liu, S. He, X. Dong, J. Zhang, H. Wang, C. Dong, M. Fang, X. Wang, Q. Peng, Z. Wang, S. Zhang, F. Yang, Z. Xu, C. Chen, and X. J. Zhou, Phys. Rev. Lett. **106**, 107001 (2011).
- <sup>23</sup> X.-P. Wang, T. Qian, P. Richard, P. Zhang, J. Dong, H.-D. Wang, C.-H. Dong, M.-H. Fang, H. Ding Europhysics Letters **93**, 57001 (2011).
- <sup>24</sup> J. T. Park, G. Friemel, Y. Li, J.-H. Kim, V. Tsurkan, J. Deisenhofer, H.-A. Krug von Nidda, A. Loidl, A. Ivanov, B. Keimer, and D. S. Inosov, Phys. Rev. Lett. **107**, 177005 (2011).
- <sup>25</sup> M. Eimenkel and K. B. Efetov, Phys. Rev. B **84**, 214508 (2011).
- <sup>26</sup> X. Dai, Z. Fang, Y. Zhou, F.-C. Zhang, Phys. Rev. Lett. **101**, 057008 (2008).
- <sup>27</sup> I.I. Mazin, M.D. Johannes, L. Boeri, K. Koepernik, D.J. Singh, Phys. Rev. B **78**, 085104 (2008).
- <sup>28</sup> J. T. Park, D. S. Inosov, A. Yaresko, S. Graser, D. L. Sun, Ph. Bourges, Y. Sidis, Yuan Li, J.-H. Kim, D. Haug, A. Ivanov, K. Hradil, A. Schneidewind, P. Link, E. Faulhaber, I. Glavatsky, C. T. Lin, B. Keimer, V. Hinkov, Phys. Rev. B **82**, 134503 (2010)
- <sup>29</sup> For circular pockets, the interaction Hamiltonian (3) is expressed via the square of the total charge density,  $n = c_\alpha^\dagger c_\alpha + d_\alpha^\dagger d_\alpha$ , total  $\mathbf{S}^2$ , where  $\mathbf{S} = (1/2)(c_\alpha^\dagger c_\beta + d_\alpha^\dagger d_\beta)\sigma_{\alpha\beta}$ , and  $O(2)$  and  $SU(2)$ -invariant combination  $\tilde{n}^2$ , where  $\tilde{n} = c_\alpha^\dagger d_\alpha - d_\alpha^\dagger c_\alpha$ , as  $H = (U)n^2/2 + J'\tilde{n}^2/2 + 2J\mathbf{S}^2$ . The interactions  $u_i$  in (3) are  $u_1 = U - 3J, u_2 = -2J - J', u_3 = J', u_4 = U - 3J$ . Then  $u_4 - u_3 = u_1 + u_2 = U - 3J - J'$ .
- <sup>30</sup> See Supplementary material.
- <sup>31</sup> Our scenario for  $s + id$  state is different from the one proposed by C. Platt, R. Thomale, C. Honerkamp, S.-C. Zhang, and W. Hanke, arXiv:1106.5964. They found a sliver of  $s + id$  state in systems with hole and electron pockets, due to competition between intra-pocket  $s$  and  $d$  pairing.
- <sup>32</sup> The pairing problem at  $k_z = \pi/2$  generally involves four sets of fermions at  $(\pi, 0, \pm\pi/2)$  and  $(0, \pi, \pm\pi/2)$ , of which two pairs hybridize and all four fermions interact with each other. This problem is equivalent to our 2D problem if the interaction is peaked at  $k_z = \pi$  because then the pairing problem decouples into two independent sets, each contains a pair of fermions, like in our 2D analysis.
- <sup>33</sup> M. Yamashita, Y. Senshu, T. Shibauchi, S. Kasahara, K. Hashimoto, D. Watanabe, H. Ikeda, T. Terashima, I. Vekhter, A. B. Vorontsov, Y. Matsuda, Phys. Rev. B **84**, 060507(R) (2011).
- <sup>34</sup> I. I. Mazin, T. P. Devereaux, J. G. Analytis, Jiun-Haw Chu, I. R. Fisher, B. Muschler, and R.

Hackl, Phys. Rev. B 82, 180502(R) (2010).

<sup>35</sup> M.M. Korshunov, and I. Eremin, Phys. Rev. B **78**, 140509(R) (2008).

<sup>36</sup> T.A. Maier, and D.J. Scalapino, Phys. Rev. B **78**, 020514(R) (2008).

## I. SUPPLEMENTARY MATERIAL

In this supplement we present the calculations that were quoted in the main text.

### A. Circular Fermi pockets

In this case  $\cos 2\theta = 0$ ,  $\sin 2\theta = 1$  and the interaction Eqs. (11), (12) simplifies,

$$H = -2u_s[J_-^\dagger]_{\sigma\sigma'}[J_-]_{\sigma'\sigma} - 2u_d[\tilde{J}_+^\dagger]_{\sigma\sigma'}[\tilde{J}_+]_{\sigma'\sigma}. \quad (15)$$

With  $u_s = u_d = u$  the inter- and intra-band order parameters are degenerate at  $\lambda = 0$  as under the above  $O(2)$  operations these two order parameters transform through each other. At finite  $\lambda$  the intra-band order should form first upon cooling as Cooper logarithms in this channel in contrast to inter-band pairing are unaffected by hybridization. In terms of anomalous averages  $2\Delta_s = \langle a_\uparrow^\dagger a_\downarrow^\dagger \rangle - \langle b_\uparrow^\dagger b_\downarrow^\dagger \rangle$ ,  $2\Delta_d = \langle a_\uparrow^\dagger b_\downarrow^\dagger \rangle + \langle b_\uparrow^\dagger a_\downarrow^\dagger \rangle$  non-linear mean field equations obtained from (15) reads

$$1 = 2uT \sum_n \frac{\pi}{\sqrt{4u^2\Delta_s^2 + \epsilon_n^2}}. \quad (16)$$

The linearized mean field equation on  $\Delta_d$  at finite  $\Delta_s$  takes the form

$$1 = 2uT \sum_n \frac{\pi}{\sqrt{4u^2\Delta_s^2 + \epsilon_n^2}} \frac{4u^2\Delta_s^2 + \epsilon_n^2}{4u^2\Delta_s^2 + \epsilon_n^2 + \lambda^2}. \quad (17)$$

It follows from comparison of (16) and (17) that once the  $s$ -wave order sets in, the  $d$ -wave order is preempted. This is a consequence of circular shape of Fermi pockets.

In the case of elliptical pockets and zero hybridization, the order parameter has opposite sign at two pockets, what implies a  $d$ -wave symmetry. The hybridization, which favors  $s$ -wave phase then competes with eccentricity which favors  $d$ -wave phase.

## B. Evaluation of the Ginzburg-Landau Functional

To map a phase diagram in the  $(\kappa, T)$ -plane we derive the Ginzburg-Landau Functional (GLF). We follow standard steps – Hubbard-Stratonovitch decoupling in Cooper channel and integration over fermion fields, and obtain the expression for the free energy

$$F[\Delta_s, \Delta_d] = -T \sum_{kn} \log \det [G_{k,n}^{-1}] + \frac{|\Delta_s|^2}{u_s} + \frac{|\Delta_d|^2}{u_d}, \quad (18)$$

where the inverse Green function is

$$G_{k,n}^{-1} = \begin{bmatrix} -(G_{kn,+}^a)^{-1} & c\Delta_d + s\Delta_s & 0 & -s\Delta_d + c\Delta_s \\ c\Delta_d^* + s\Delta_s^* & (G_{kn,-}^a)^{-1} & -s\Delta_d^* + c\Delta_s^* & 0 \\ 0 & -s\Delta_d + c\Delta_s & -(G_{kn,+}^b)^{-1} & -c\Delta_d - s\Delta_s \\ -s\Delta_d^* + c\Delta_s^* & 0 & -c\Delta_d^* - s\Delta_s^* & (G_{kn,-}^b)^{-1} \end{bmatrix}. \quad (19)$$

In the last equation the free Green functions are  $G_{kn,\pm}^{a(b)} = (\pm i\epsilon_n - \xi_{\pm k}^{a(b)})^{-1}$ ,  $\xi_k^{a,b} = E_k^{a,b} - \epsilon_F$ .

Expansion of Eq. (18) to fourth order yields GLF in the form

$$F_{GL} = A_s |\Delta_s|^2 + A_d |\Delta_d|^2 + \frac{B_s}{2} |\Delta_s|^4 + \frac{B_d}{2} |\Delta_d|^4 \\ + C |\Delta_s|^2 |\Delta_d|^2 + \frac{E_1}{2} (\Delta_s \Delta_d^*)^2 + \frac{E_2}{2} (\Delta_s^* \Delta_d)^2. \quad (20)$$

The expressions for  $A_s$  and  $A_d$  are

$$A_s = \frac{1}{u} - T \sum_{kn} [s^2 (G_-^a G_+^a + G_-^b G_+^b) + c^2 (G_-^a G_+^b + G_+^a G_-^b)] \quad (21)$$

and  $A_d$  is obtained from (21) by exchanging  $c \leftrightarrow s$ . Observe that Eq. (21) contains both intra- and intra-band contributions. They correspond to first and second terms in the square brackets, respectively.

The expressions for the other coefficients in terms of fermion propagators are

$$B_s = T \sum_{kn} \left[ s^4 ((G_-^a)^2 (G_+^a)^2 + (G_+^b)^2 (G_-^b)^2) + c^4 ((G_-^a)^2 (G_+^b)^2 + (G_+^a)^2 (G_-^b)^2) \right. \\ \left. + 2c^2 s^2 (G_+^a (G_-^a)^2 G_+^b + G_+^a G_+^b (G_-^b)^2 + G_-^a (G_+^a)^2 G_-^b + G_-^a (G_+^b)^2 G_-^b - 2G_-^a G_+^a G_-^b G_+^b) \right]. \quad (22)$$

The expression for the parameter  $B_d$  is obtained from Eq. (22) by interchanging  $s \leftrightarrow c$ .



Further,

$$\begin{aligned}
C = T \sum_{kn} & \left[ (c^4 + s^4) (G_a^+ (G_a^-)^2 G_b^+ + G_a^+ G_b^+ (G_b^-)^2 + (G_a^+)^2 G_a^- G_b^- + G_a^- (G_b^+)^2 G_b^-) \right. \\
& + 2c^2 s^2 ((G_a^+)^2 (G_a^-)^2 + (G_a^-)^2 (G_b^+)^2 - G_a^+ (G_a^-)^2 G_b^+ + (G_a^+)^2 (G_b^-)^2 \\
& \left. + (G_b^+)^2 (G_b^-)^2 - G_a^+ G_b^+ (G_b^-)^2 - (G_a^+)^2 G_a^- G_b^- - G_a^- (G_b^+)^2 G_b^- + 4G_a^+ G_a^- G_b^+ G_b^-) \right], \quad (23)
\end{aligned}$$

$$\begin{aligned}
E_1 = E_2 = E = T \sum_{kn} & \left[ -2(c^4 + s^4) G_a^+ G_a^- G_b^+ G_b^- \right. \\
& + c^2 s^2 ((G_a^+)^2 (G_a^-)^2 + (G_a^-)^2 (G_b^+)^2 - 2G_a^+ (G_a^-)^2 G_b^+ + (G_a^+)^2 (G_b^-)^2 \\
& \left. + (G_b^+)^2 (G_b^-)^2 - 2G_a^+ G_b^+ (G_b^-)^2 - 2(G_a^+)^2 G_a^- G_b^- - 2G_a^- (G_b^+)^2 G_b^-) \right]. \quad (24)
\end{aligned}$$

The evaluation of GLF parameters simplifies in two limiting cases. At  $T_c^* \ll \lambda$  only the terms with propagators of particles from the same band, like the first two terms in Eq. (22), are important in (21), (22), (23) and (24). The parameters of the quadratic part of the GLF read

$$A_{s(d)} = \frac{1}{u} - f_{s(d)}(\kappa) \log \frac{\Lambda}{T}, \quad (25)$$

where  $f_s(\kappa) = \langle \sin^2 2\theta_k \rangle$ ,  $f_d = 1 - f_s$ ,  $\sin^2 2\theta_k = \kappa^2 / (\kappa^2 + \cos^2 2\phi)$ ,  $\cos \phi = k_x / k$  and  $\langle \dots \rangle = (2\pi)^{-1} \oint d\phi \dots$ . The critical  $\kappa^* = 1/\sqrt{3}$  is obtained from the condition  $f_s(\kappa_*) = f_d(\kappa_*)$ .

### C. The case $T_c^* \gg \lambda$

For completeness, we consider the phase diagram for the case when  $T_c^* \gg \lambda$  (we recall that  $T_c^*$  is the transition temperature at the point where the lines  $A_s = 0$  and  $A_d = 0$  cross). We perform a perturbative evaluation of the GLF parameters in  $\lambda/T_c^* \ll 1$ .

Consider first the transition from normal to superconducting state. It follows from Eq. (21) that, to the leading order in  $\lambda/T_c^*$ ,  $T_{c,d} = T_{c,s}$  independent on  $\kappa$ , like in  $O(2)$  symmetric case of circular Fermi pockets. The finite difference  $\delta A = A_s - A_d$  is obtained at the second order in  $\lambda/T_c^*$ ,

$$\delta A \approx \lambda^2 \kappa^{-2} \langle \cos^2 2\phi - \kappa^2 \rangle I_0, \quad (26)$$

where  $I_0 = 7\zeta(3)/8\pi^2 T^2$ . As  $\langle \cos^2 2\phi \rangle = 1/2$ ,  $\kappa_* = 1/\sqrt{2}$ .

To evaluate the other parameters in GLF perturbatively in  $\lambda/T_c$  we write  $\xi_{a,b} = \xi \pm \delta E$ ,  $\delta E \approx \lambda \kappa^{-1} \sqrt{\kappa^2 + \cos^2 2\phi} \ll \xi \sim T_c$  and expand Green functions in  $\delta E$ . Substituting the expansion in Eqs. (22), (23) and (24) we obtain  $B_s^{(0)} = B_d^{(0)} = 2I_0$ ,  $C^{(0)} = 4I_0$ ,  $E_1^{(0)} = E_2^{(0)} = -2I_0$ . Because  $E_{1,2}^{(0)} < 0$  we write the quartic part of GLF in the form

$$F^{(4)} \approx \frac{B^{(0)}}{2}(|\Delta_s|^2 + |\Delta_d|^2)^2 + (C^{(0)} - B^{(0)} + E^{(0)})|\Delta_s|^2|\Delta_d|^2 + \frac{E^{(0)}}{2}(\Delta_s\Delta_d^* - \Delta_s^*\Delta_d)^2. \quad (27)$$

The GLF is at minimum when  $\Delta_s$  and  $\Delta_d$  are in phase, i.e., time-reversal symmetry is not

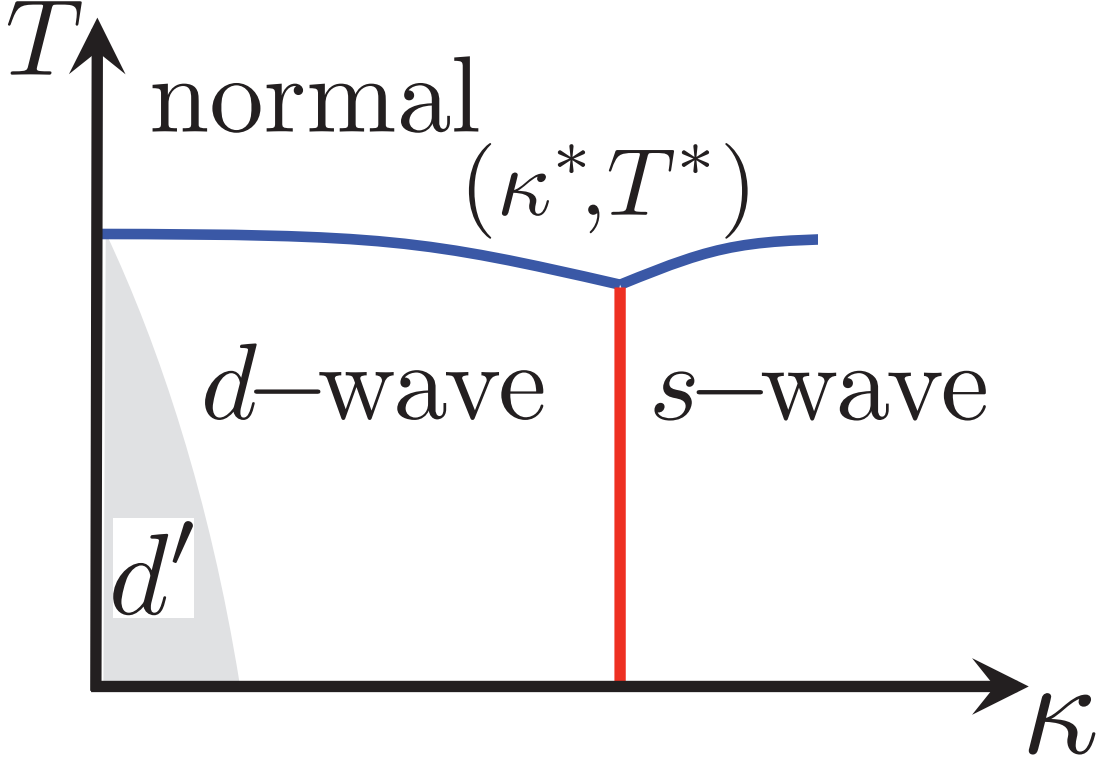


FIG. 5: Phase diagram in the  $(\kappa, T)$ -plane for  $T_c^* \gg \lambda$ . There is still a transformation from  $d$ -wave to  $s$ -wave gap symmetry as  $\kappa$  increases, but the two phases are now separated by first-order transition. There is no intermediate  $s + id$  phase. Within the  $d$ -wave phase, there is still a region (dubbed as  $d'$ ) where the gap has no nodes.

broken in the strong coupling limit. Still the leading order expansion is not sufficient to determine whether the intermediate phase of an  $s + d$  symmetry exists because  $C^{(0)} - B^{(0)} + E^{(0)} = 0$ . It turns out that at the second order GLF is still degenerate,  $C^{(2)} - \sqrt{B_s^{(2)} B_d^{(2)}} + E^{(2)} = 0$ , hence we higher order expansion. We obtained up to the fourth order in  $\lambda/T_c$

found that  $C - \sqrt{B_s B_d} + E$  is positive:

$$C - \sqrt{B_s B_d} + E \approx C^{(4)} - \frac{1}{2}(B_s^{(4)} + B_d^{(4)}) + E^{(4)} = T \sum_n \int d\xi \frac{7(\delta E)^4}{(\epsilon_n^2 + \xi^2)^4}. \quad (28)$$

This implies that at strong coupling,  $s$ -wave and  $d$ -wave phases are separated by first order transition line. We show the phase diagram for  $T_c^* \gg \lambda$  in Fig. 5.